Limnol. Oceanogr., 45(6), 2000, 1224–1234

The fate of intertidal microphytobenthos carbon: An in situ ^{13}C-labeling study

Jack J. Middelburg[1]
Netherlands Institute of Ecology, P.O. Box 140, 4400 AC Yerseke, The Netherlands

Christiane Barranguet
University of Amsterdam, Department of Aquatic Ecology and Ecotoxicology, Kruislaan 320, 1098 SM Amsterdam, The Netherlands

Henricus T. S. Boschker and Peter M. J. Herman
Netherlands Institute of Ecology, P.O. Box 140, 4400 AC Yerseke, The Netherlands

Tom Moens
University of Gent, Biology Department, Marine Biology Section, K. L. Ledeganckstraat 35, 9000 Gent, Belgium

Carlo H. R. Heip
Netherlands Institute of Ecology, P.O. Box 140, 4400 AC Yerseke, The Netherlands

Abstract

At two intertidal sites (one sandy and one silty, in the Scheldt estuary, The Netherlands), the fate of microphytobenthos was studied through an in situ ^{13}C pulse-chase experiment. Label was added at the beginning of low tide, and uptake of ^{13}C by algae was linear during the whole period of tidal exposure (about 27 mg m^{-2} h^{-1} in the top millimeter at both sites). The ^{13}C fixed by microphytobenthos was rapidly displaced toward deeper sediment layers (down to 6 cm), in particular at the dynamic, sandy site. The residence times of microphytobenthos with respect to external losses (resuspension and respiration) were about 2.4 and 5.6 d at the sandy and silty stations, respectively. The transfer of carbon from microphytobenthos to benthic consumers was estimated from the appearance of ^{13}C in bacterial biomarkers, handpicked nematodes, and macrofauna. The incorporation of ^{13}C into bacterial biomass was quantified by carbon isotope analysis of polar lipid derived fatty acids specific for bacteria. The bacterial polar lipid-derived fatty acids (i14:0, i15:0, a15:0, i16:0, and 18:1ω7c) showed rapid, significant transfer from benthic algae to bacteria with maximum labeling after 1 d. Nematodes became enriched after 1 h, and ^{13}C assimilation increased until day 3. Microphytobenthos carbon entered all heterotrophic components in proportion to heterotrophic biomass distribution (bacteria > macrofauna > meiofauna). Our results indicate a central role for microphytobenthos in moderating carbon flow in coastal sediments.

Microphytobenthos, the microscopic photosynthetic organisms living on the sediment surface, contribute significantly to the total primary production of estuarine and other shallow water ecosystems (MacIntyre et al. 1996; Underwood and Kromkamp 1999). These benthic algae are consequently an important carbon source for benthic heterotrophs (Herman et al. 1999) and can significantly affect the exchange of oxygen and nutrients across the sediment–water interface (Risgaard-Petersen et al. 1994). Microphytobenthos, particularly diatoms and cyanobacteria, have been reported to stabilize the sediment surface against resuspension by the extrusion of extracellular polymeric substances (Holland et al. 1974; Paterson and Black 1999). Although the importance of microphytobenthos to the functioning of shallow ecosystems has been well established (Heip et al. 1995) and biomass and light availability have been recognized as the principal factors determining microphytobenthos production (MacIntyre et al. 1996; Underwood and Kromkamp 1999), there is little information on its fate. The microalgae living in the top few millimeters of the sediment may be resuspended, mixed to deeper layers, or consumed by heterotrophs.

Turbulence and shear stress generated by waves or tidal currents may cause resuspension of surface sediments and associated microphytobenthos (de Jonge and van Beusekom 1995). Resuspension lowers biomass, hence the potential production of microphytobenthos. Resuspended microphytobenthos may contribute significantly to water column production (MacIntyre and Cullen 1995) and constitute an important food source for suspension feeders (Herman et al. 1999). Ripple movement and sediment mixing due to tidal currents, waves, and bioturbation may displace algae from surface layers to depths of more than 10 cm (Steele and

[1] Corresponding author (Middelburg@cemo.nioo.knaw.nl).

Acknowledgments

We thank Bernard Krebs, Piet de Koeijer, Myriam Beghyn, and Annick Van Kenhove for assistance with macro and meiofauna sample processing. We thank Maaike Steyaert for providing nematode biomass data, Joop Nieuwenhuize for analytical assistance, and two anonymous reviewers for constructive remarks. This is a contribution of the project ECOFLAT (ENV 4-CT96-0216) to the EU ELOISE program and publication 2649 of the Netherlands Institute of Ecology.

Baird 1968; Cadee and Hegeman 1974). These algae that occur far below the euphotic zone usually exhibit photosynthetic activity (Steele and Baird 1968).

It has been well established that grazing by micro-, meio-, and macrofauna may affect microphytobenthos biomass, but most studies have been limited to a single or a few consumer species and have been performed in laboratory or experimental systems rather than in situ (Miller et al. 1996). Unbalanced growth of microphytobenthos may cause release of photosynthesis-derived dissolved organic carbon that is used by bacteria as substrate for growth (Murray et al. 1986; Dobbs et al. 1989; Smith and Underwood 1998).

The major microphytobenthos loss pathways (resuspension, mixing and grazing, and respiration by heterotrophs) have not yet been investigated together, and quantitative information on their relative contribution is not available. In this article, we present the results of an in situ pulse-chase experiment by using ^{13}C labeling of microphytobenthos. Tidal flat sediments were labeled, and the distribution of label was used to assess the dynamics of mixing and losses. The transfer of carbon from microphytobenthos to heterotrophs was determined from ^{13}C labeling of nematodes, macrofauna, and bacterial biomarkers.

Materials and methods

Study area—In June 1997, in situ experiments were done in the Molenplaat tidal flat (51°26′N, 3°57′E), located in the midregion of the Scheldt estuary, a turbid, nutrient-rich, heterotrophic system (Fig. 1). Most of the tidal flat is located between −1 m and +1 m relative to mean tidal level and is subject to a tidal amplitude of about 5 m. The ecology of the tidal flat has been studied during the project Eco-metabolism of an estuarine tidal flat (ECOFLAT), and there is detailed background information on pigment distributions (Barranguet et al. 1997; Lucas and Holligan 1999); microphytobenthos production (Barranguet et al. 1998); photosynthetic activity (Kromkamp et al. 1998); microphytobenthos resuspension (Lucas et al. 2000); and microbenthic (Hamels et al. 1998), meiofauna (Moens et al. 1999*a*), and macrofauna (Herman et al. 2000) communities. On the basis of these data, two sites were selected, one sandy (Sta. 4) and near the edge of the flat and one silty (Sta. 2) in the center of the flat (Fig. 1). The sandy and silty stations have about 4 and 38% silt (fraction <63 μm), respectively; median grain sizes of 186 and 78 μm, respectively; and model-based maximum bottom shear stresses of 1.15 and 0.36 Pa, respectively. This difference in sediment texture is reflected in organic carbon contents of 0.07 percent dry weight (wt %) (32 g m^{-2}) and 0.70 wt% (196 g m^{-2}) in the top 5 cm at Sta. 4 and Sta. 2, respectively. The respective average oxygen uptake rates were 23 and 89 mM m^{-2} d^{-1}. These two sites represent the end members of tidal flat sediment characteristics in terms of carbon and microphytobenthos stocks, sediment dynamics, and bottom water current velocities. The experiments took place between 9 and 15 June 1997 in very bright, warm summer weather.

Labeling experiment—At the beginning of low tide, two 0.25-m^2 frames (8 cm deep) were inserted in the sediments at both stations, one being used to follow the incorporation of label during the 4.5-h period of exposure (short-term plot) and the other (long-term plot) being dedicated to trace the fate of fixed carbon over 3 (Sta. 4) to 4 (Sta. 2) d. The surface of all four plots was sprayed with 250 ml of ^{13}C-labeled bicarbonate solution (>99% ^{13}C, Isotech) with ambient salinity to obtain a final concentration of 1 g m^{-2}. The amount of ^{13}C added was based on a pilot experiment in which loadings of 0.01, 0.1, and 1 g m^{-2} were applied. The two lower levels resulted in detectable ^{13}C fixation by microphytobenthos, but these enrichments were too low to quantify transfer to heterotrophs. Replicate time zero controls were taken just outside the plots before spraying. The frequency, spatial resolution, and replication of sampling were chosen to reduce within-plot heterogeneity while preventing disturbance due to removal of material. Moreover, sampling resolution depended on the organism or pool. Sampling in each plot was based on an a priori randomized design.

The incorporation of ^{13}C was followed by collecting four 2.5-cm-diameter cores every 10 min for 4.5 h from the short-term plots. The four replicates were sliced for the superficial 1 mm and combined two by two, resulting in two pooled samples. The carbon incorporation was stopped with 100 μl

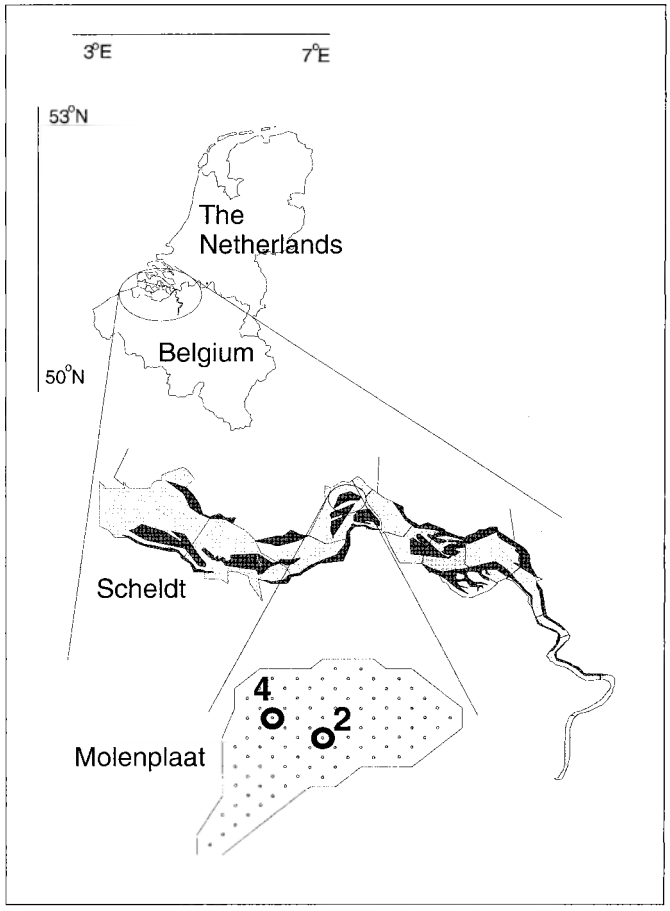

Fig. 1. Map of the study area showing the location of the Molenplaat tidal flat and the sampling locations (Sta. 2 and Sta. 4).

of concentrated HCl, and samples were stored frozen. Splits for pigment analyses were stored frozen as well (−80°C).

To study the pigment distribution and vertical distribution of ^{13}C incorporation into bulk organic matter, four replicate cores were taken from the long-term plots at the end of low tide and during daytime ebb of each of the following days. Cores were sectioned (0–1, 1–3, 3–6, 6–10, 10–20, 20–30, 30–50, and 50–70 mm), and sections were combined two by two.

For determination of ^{13}C incorporation into nematodes, replicate cores were taken from the short-term plots after 1, 2, and 4 h and from the long-term plots during daytime ebb of each of the following days. Cores were sectioned (0–10, 10–20, and 20–30 mm). Subsamples were preserved on board ship with hot (70°C) formaldehyde (final concentration 6 wt%; Moens et al. 1999*c*). No corrections were applied for any carbon added during the formaldehyde treatment. Meiofauna were elutriated with Ludox (HS40; DuPont) and resuspended in artificial seawater of ambient salinity. Nematodes were handpicked, rinsed three times in sterile artificial seawater, transferred to aluminum cups, pinched closed, and stored frozen. Nematode biomass and depth distribution data are based on data from Steyaert (pers. comm.) and refer to samples collected in June 1996. Nematode communities sampled at site four in June 1996 and in June 1997 did not differ significantly (Steyaert pers. comm.). No descriptive information on the nematode community of Sta. 2 in June 1997 is available, but here too, observations during sorting the samples of the labeling experiment suggest no significant differences from the 1996 situation.

At Sta. 2, samples were taken from the long-term plot to study the incorporation of ^{13}C in polar lipid derived fatty acids. Replicate depth profiles (0–5, 5–10, 10–15, and 15–20 mm) were recovered after 2 and 4 d, and the surface layer (0–5 mm) was sampled after 4 h and 1 and 3 d as well. All samples were extracted directly and then stored frozen.

At the end of the experiments, frames were collected, and the entire plot was sampled for macrofauna. The sediment was sliced (0–2, 2–4, 4–9, and 9–14 cm), washed over a 0.5-mm sieve, and immediately sorted on the species level. Macrofauna biomass and its depth distribution are based on the collection of 10 cores with a diameter of 10 cm just outside the plots. The specific uptake rates of individual macrofauna species will be presented elsewhere (Herman et al. 2000).

Microphytobenthos production—Microphytobenthos production was based on ^{14}C uptake in slurries incubated in replicate at various light levels and in the dark and assuming an exponential decrease of light intensity in the sediments (MacIntyre and Cullen 1995; Barranguet et al. 1998). Three photosynthesis versus irradiance (P-I) curves were determined, because photosynthetic parameters may change during the period of exposure (Kromkamp et al. 1998). The euphotic zones (>1% ambient light) were 2.6 and 1.0 mm at Sta. 4 and Sta. 2, respectively.

Analytical techniques—Pigments were extracted from freeze-dried samples with methanol (95%), buffered with ammonium acetate (5%), and analyzed by reverse-phase high-performance liquid chromatography (Barranguet et al. 1997, 1998). Results are expressed in milligrams of chlorophyll *a* (Chl *a*) per square meter. Freeze-dried sediment samples were analyzed for organic carbon by using a Carlo Erba elemental analyzer following an in situ acidification procedure. The carbon isotopic composition of sediments and handpicked organisms was determined using a Fisons CN elemental analyzer coupled on-line, via a Finnigan conflo 2 interface, with a Finnigan Delta S mass spectrometer. Reproducibility of $\delta^{13}C$ values was better than 0.1‰.

Lipids were extracted from 3 g wet weight of sediment with a modified Bligh and Dyer extraction (Boschker et al. 1999). The lipid extract was fractionated on silicic acid (60, Merck) into different polarity classes by sequential eluting with chloroform, acetone, and methanol. The methanol fraction containing the phospholipid ester-linked fatty acids (PLFA) was derivatized using mild alkaline methanolysis to yield fatty acid methyl esters (FAME). Internal FAME standards of both 12 : 0 and 19 : 0 were used. Identification of FAME was based on the comparison of retention time data with known standards on two analytical columns with different polarities (*see below*). Additional identification was gained by gas chromatography–mass spectrometry on a Hewlett-Packard mass selective detector (HP 5970). PLFA shorthand nomenclature is according to Guckert et al. (1985). FAME concentrations were determined by gas chromatography-flame ionisation detection (GC-FID).

The isotopic composition of individual FAME was determined using a Varian 3400 gas chromatograph equipped with a Varian SPI injector, which was coupled via a type II combustion interface to a Finnigan Delta S isotope ratio mass spectrometer. A polar analytical column (Scientific Glass Engineering BPX-70, 50 m × 0.32 mm × 0.25 μm) was used with helium as carrier gas. The column was kept at 80°C for 1 min, then temperature was programmed from 80 to 130°C at 40°C min^{-1} and subsequently from 130 to 240°C at 3°C min^{-1}. Several samples were also analyzed on an apolar column (Hewlett-Packard Ultra-2, 50 m × 0.32 mm × 0.17 μm) under similar conditions. Stable carbon isotope ratios for individual FAME, as determined on both analytical columns, were similar. To obtain the actual PLFA ratio, carbon isotope ratios of FAME were corrected by using a mass balance for the one carbon atom in the methyl group that was added during derivatization. The methanol that was used for derivatization had a ratio of −45.6 ± 0.9‰ (N = 4), as determined by gas chromatography-isotope ratio mass spectroscopy (GC-IRMS). Reproducibility of PLFA isotopic measurements was better than 1‰.

Data treatment—Incorporation of ^{13}C is reflected as excess (above background) ^{13}C and is expressed in terms of total uptake (I) in milligrams of ^{13}C per square meter as well as specific uptake (i.e., $\Delta\delta^{13}C = \delta^{13}C_{sample} - \delta^{13}C_{control}$, where $\delta^{13}C$ is expressed relative to Vienna Pee Dee Belemnite (PDB)). I was calculated as the product of excess ^{13}C (E) and organic carbon, biomass, or PLFA carbon. Excess ^{13}C is the difference between the fraction ^{13}C of the control ($F_{control}$) and the sample (F_{sample}): $E = F_{sample} - F_{control}$, where $F = {}^{13}C/({}^{13}C + {}^{12}C) = R/(R + 1)$. The carbon isotope ratio (R) was

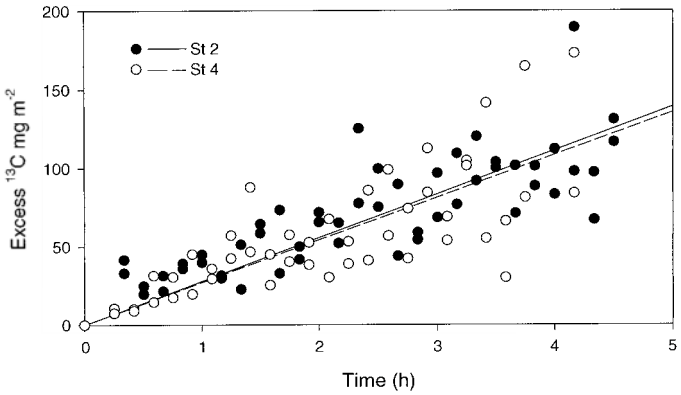

Fig. 2. Linear uptake of ^{13}C by sediment microalgae in the top millimeter as a function of incubation time. Slopes of regression lines correspond to uptake rates of 27.8 ± 1.1 and 27.1 ± 1.6 milligrams of ^{13}C per square meter per hour at Sta. 2 and Sta. 4, respectively.

derived from the measured δ^{13}C values as $R = (\delta^{13}C/1000 + 1) \times R_{VPDB}$, with $R_{VPDB} = 0.0112372$.

Label incorporation into bacterial biomass was calculated from the label in bacterial PLFA (i14:0, i15:0, a15:0, i16:0, and 18:1ω7c) as

$$I_{bact} = \sum I_{PLFAbact}/(a \times b),$$

where a is the average PLFA concentration in bacteria (0.056 g of carbon PLFA per gram of carbon biomass; Brinch-Iversen and King 1990), and b is the average fraction-specific bacterial PLFA encountered in sediments dominated by bacteria (0.28 ± 0.04; calculated from Rajendran et al. 1993, 1994; Guezennec and Fialamedioni 1996; Steward et al. 1996; and Boschker et al. 1998). Label incorporation into algae was calculated from the difference between the label incorporation into all PLFA and into the bacterial PLFA as

$$I_{algae} = \left(\sum I_{PFLAall} - \sum I_{PLFAbact}\right)/c.$$

The average PLFA concentration in diatoms (c = 0.035 g of carbon PLFA per gram of carbon biomass) was calculated from the data presented in Volkman et al. (1989) and Brinch-Iversen and King (1990) with the assumption that the carbon to Chl *a* ratio was 40.

Data are reported as the mean with standard deviation rather than standard error to better reflect the heterogeneity of the microphytobenthos distribution. Combined errors are based on standard error propagation procedures assuming independence of errors.

Results

In the top millimeter of sediments incorporation of excess (above background), ^{13}C was linear over more than 4 h and was similar at the two stations: 27.8 ± 1.1 and 27.1 ± 1.6 mg m^{-2} h^{-1} at Sta. 2 and Sta. 4, respectively (Fig. 2). Variability of replicates increased with time, but the residuals were not correlated to Chl *a* or organic carbon concentrations. Chl *a* concentrations in the top millimeter averaged 39.2 ± 10.4 and 5.1 ± 2.7 mg m^{-2} at Sta. 2 and Sta. 4, respectively, and did not increase with time. At the end of the labeling period, the quantities of ^{13}C fixed in the top millimeter at the short-term and long-term plots were comparable, namely 104.7 ± 32.2 and 80.5 ± 0.9 mg m^{-2} at Sta. 2 and 125.7 ± 49.9 and 85.5 ± 71.8 mg m^{-2} at Sta. 4. ^{14}C uptake rates in slurries from the top millimeter of the sediment varied from the start to end of exposure: 107 to 48 mg m^{-2} h^{-1} at Sta. 2 and 59 to 102 mg m^{-2} h^{-1} at Sta. 4. Depth-integrated rates of ^{13}C fixation were 32 ± 4 and 60 ± 9 mg m^{-2} h^{-1} at Sta. 2 and Sta. 4, respectively, and were lower than the respective whole photic zone carbon uptake based on slurry ^{14}C uptake: 49–108 and 66–112 mg m^{-2} h^{-1}.

At the end of the labeling period, about 25% of the label was found at a depth of more than 1 mm at Sta. 2 and about 60% at Sta. 4. This larger depth penetration at Sta. 4 relative to Sta. 2 is consistent with the larger euphotic zone depth (2.6 vs. 1 mm, respectively). During the consecutive days, there was rapid and extensive transfer of ^{13}C-labeled organic matter to deeper layers (Fig. 3). Consistently, intact Chl *a* was found to the maximum sampling depth, well below the euphotic zone. The slope of the weighted log-linear regression of Chl *a* with depth was steeper at Sta. 4 (−0.022 ± 0.003) than at Sta. 2 (−0.013 ± 0.002; Fig. 3C), and depth-integrated concentrations of Chl *a* at Sta. 4 (14 ± 1.6 mg m^{-2}) were lower than those at Sta. 2 (52 ± 10.5 mg m^{-2}).

Inventories of ^{13}C were estimated by integration of ^{13}C stocks to the maximum depth of sampling. Inventories ranged from 150 to 60 mg and 250 to 90 mg m^{-2} at Sta. 2 and Sta. 4, respectively, and they decreased with time (Fig. 4). The half-life of ^{13}C (ln2/attenuation coefficient) with respect to external losses (resuspension, respiration, and mixing to below maximum sampling depth) were 5.6 and 2.4 d at Sta. 2 and Sta. 4, respectively.

Sample requirement for mass spectrometry on the one hand and sample size and nematode biomass on the other hand did not allow us to separate nematodes at the genus level, except at Sta. 4, where the dominant large predatory nematode *Enoploides longispiculosus* was separated from the other nematodes. Label uptake is expressed as an enrichment ($\Delta\delta^{13}$C) relative to the control at time zero (δ^{13}C: −18.0 ± 1.0 and −15.2‰ at Sta. 2 and Sta. 4, respectively, and −14.3 ± 1.4‰ for *E. longispiculosus*). Enrichment in ^{13}C of nematodes became apparent after 1 h and increased until day 3 (Fig. 5A,B). It appears that there is delayed or no uptake of ^{13}C during the period 4 to 24 h after labeling. Uptake patterns of *E. longispiculosus* were similar, but the delay in uptake during the period 4 to 24 h after labeling was more pronounced, and more of the label was found in the deeper layers (Fig. 5C). The final quantities of label incorporated in nematodes biomass were 0.19 and 0.54 mg m^{-2} at Sta. 2 and Sta. 4, respectively, the difference being related to differences in carbon in biomass (0.18 and 0.62 g m^{-2}, respectively; Fig. 5D).

Macrofauna was separated at the species level, and the ^{13}C enrichment of the organisms relative to the control after 3 (Sta. 4) and 4 d (Sta. 2) has been determined. *Nereis succinea, Pygospio elegans,* and *Macoma balthica* were strongly enriched ($\Delta\delta^{13}C > 20‰$), whereas the other organisms showed less enrichment (Herman et al. 2000). Macrofauna

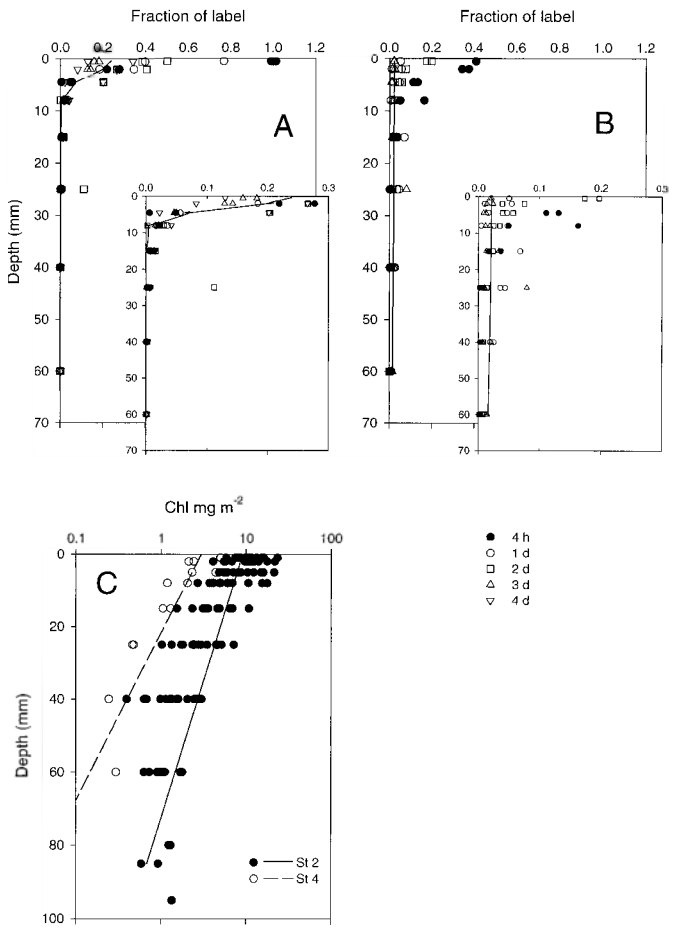

Fig. 3. The fraction of excess ^{13}C as a function of depth at (A) Sta. 2 and (B) Sta. 4. The fraction of excess ^{13}C has been calculated by dividing the concentration of excess ^{13}C with the concentration of excess ^{13}C in the top millimeter at the end of the labeling period. Expanded fraction scales are shown in the insets. The solid lines represent best fits of pulse-deposition-diffusion-loss models, with D values of 4 and 3880 $cm^2\ yr^{-1}$ and k values of 0.02 and 0.05 h^{-1} at Sta. 2 and Sta. 4, respectively. (C) Depth profiles of Chlorophyll *a* with weighted log-linear regression lines having slopes of -0.013 ± 0.002 and -0.022 ± 0.003 at Sta. 2 and Sta. 4 have also been indicated.

carbon biomass was 9.6 and 10.2 g m^{-2} at Sta. 2 and Sta. 4 and accounted for 4.4 and 8 mg m^{-2}, respectively.

The PLFA concentration patterns were dominated by C16:0, C16:1ω7c, C18:1ω7c, C20:4ω6, C20:5ω3, and C22:6ω3 (*see Fig. 6A for an example*). Some PLFA (C14:0, C16:2ω4, C18:2ω6c, C18:3ω6, C18:3ω3, C18:4ω3, and C20:4ω3) were strongly enriched after 4 h ($\Delta\delta^{13}C > 1{,}000‰$), and their specific uptake decreased steadily with time (Fig. 6C–E). Other PLFA (C16:0, C16:1ω7c, C16:3ω4, and C20:5ω3) also became enriched in ^{13}C after 4 h, but their specific labeling remained rather constant for about 2 d. The bacterial biomarkers (i14:0, i15:0, a15:0, i16:0, and 18:1ω7c) showed maximal specific uptake at days 1 and 2 (Fig. 6D) and had very low concentrations, except for 18:1ω7c. Incorporation patterns after 4 h were very similar to PLFA patterns of diatoms; thereafter, bacterial biomarkers and some general

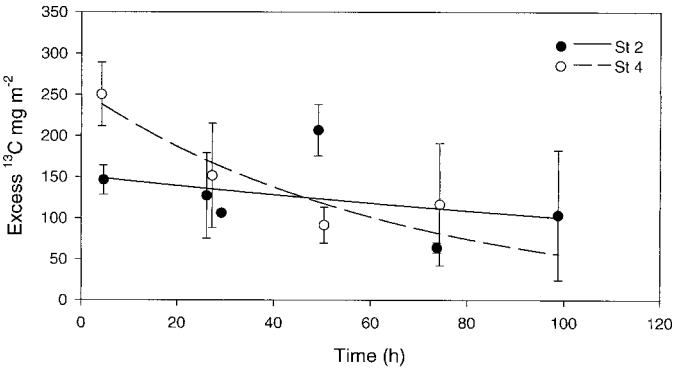

Fig. 4. Excess ^{13}C inventory as a function of time. Exponential fits with attenuation coefficients of -0.0052 ± 0.005 (Sta. 2) and -0.012 ± 0.005 (Sta. 4) have been indicated as well. Error bars represent standard deviations.

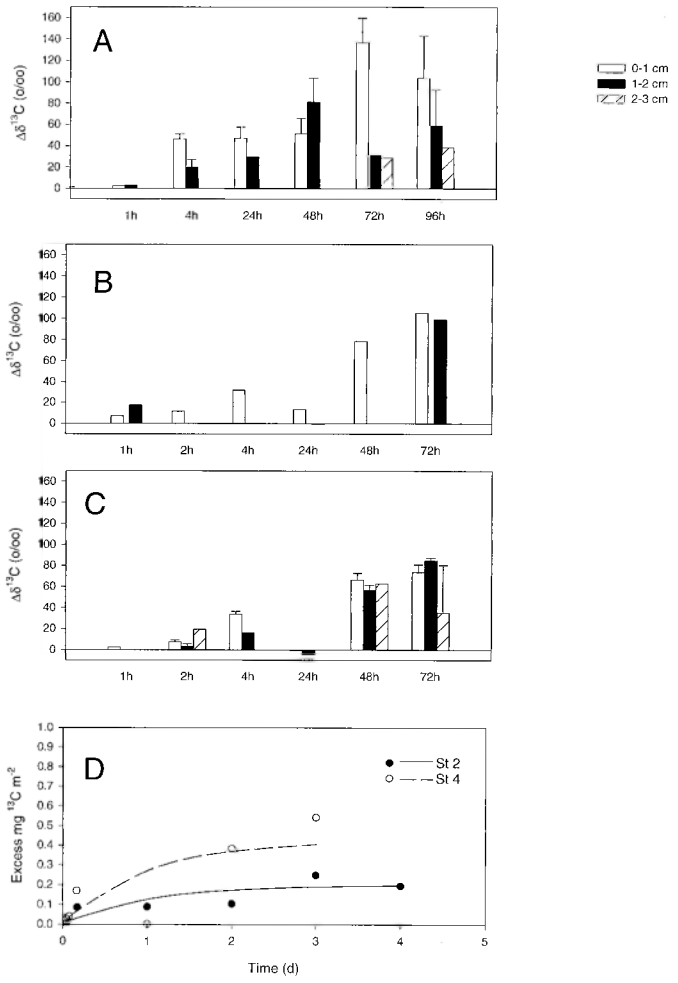

Fig. 5. (A) Specific uptake ($\Delta\delta^{13}C$) by nematode community at Sta. 2. (B) Specific uptake ($\Delta\delta^{13}C$) by nematode community (except *Enoploides longispiculosus*) at Sta. 4. (C) Specific uptake ($\Delta\delta^{13}C$) by *Enoploides longispiculosus* at Sta. 4. Error bars represent the standard deviations. (D) Assimilation of ^{13}C by nematode communities at Sta. 2 and Sta. 4. Assimilation has been fitted to $A = A_0[1-\exp(-kt)]$, with A_0 values of 0.2 and 0.43 mg m^{-2} and k values of 0.98 and 1.0 d^{-1} at Sta. 2 and Sta. 4, respectively.

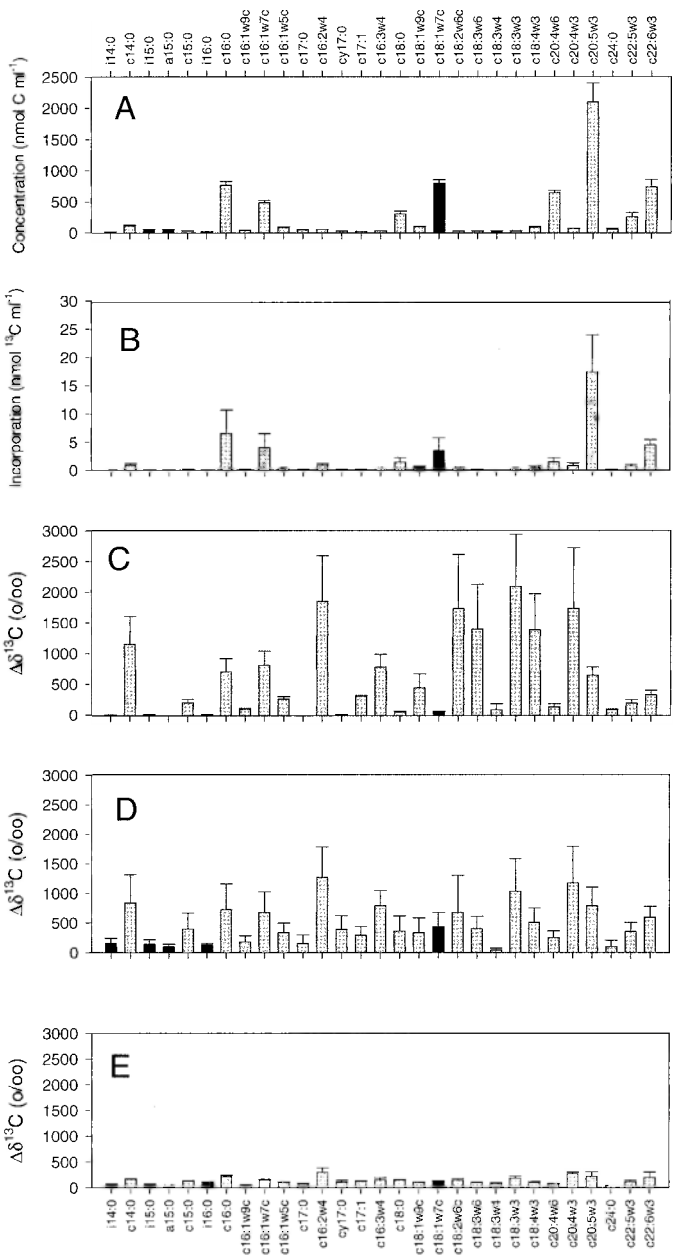

Fig. 6. (A) Concentrations of individual PLFA (4-h example). (B) ^{13}C incorporation in PLFA after 2 d. (C–E) Specific labeling patterns of PLFA ($\Delta\delta^{13}C$) after 4 h, 2 d, and 4 d. Error bars represent standard deviations. Solid bars show bacterial PLFA.

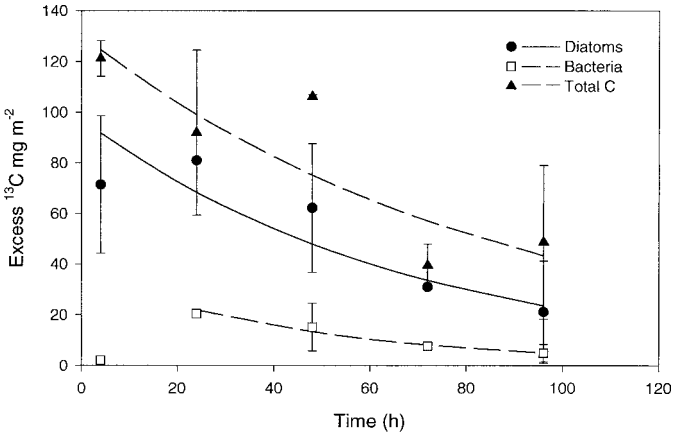

Fig. 7. Evolution of excess ^{13}C in the pools of total carbon, diatom, and bacterial biomass in the top 5 mm at Sta. 2. The error bars represent standard deviations. Exponential fits with attenuation coefficients of -0.0012 ± 0.004 (total carbon), -0.015 ± 0.003 (diatom), and -0.021 ± 0.002 (bacteria) have been indicated as well.

PLFA (18 : 0) contributed as well (data not shown). During the whole period, incorporation patterns were dominated by C16:0, C16:1ω7c, C20:5ω3, and C22:6ω3 because of their high concentrations (*see Fig. 6B for an example*). Bacterial and diatom (16:2ω4, 20:5ω3, and 22:6ω3) PLFA at time zero had $\delta^{13}C$ values of -20.3 ± 1.9 and -21.6 ± 1.9‰, respectively. These PLFA are likely isotopically depleted compared to the total biomass and the substrate used by the bacteria (e.g., Boschker et al. 1999).

The partitioning of fixed ^{13}C and its evolution with time in the top 5 mm of the sediment at Sta. 2 is shown in Fig. 7. At the end of the labeling period, 71 ± 27 mg m^{-2} was incorporated in diatoms (59%), 2.1 ± 0.6 mg m^{-2} in bacteria (1.7%), and the remaining 39% (47 ± 28 mg m^{-2}) in other compartments. The total and algal ^{13}C inventories in the top 5 mm subsequently decreased exponentially with attenuation coefficients of 0.012 ± 0.004 and 0.015 ± 0.003 h^{-1}, corresponding to half-lives of 2.5 and 1.9 d, respectively. During the first 24 h, the incorporation of ^{13}C in bacterial biomass increased to a maximum of about 20 mg m^{-2} and then exponentially decreased with an attenuation coefficient of 0.021 ± 0.002 h^{-1} (half-life of 1.4 d).

The partitioning of ^{13}C among the different benthic size classes can be made only at days 2 and 4 for the top 20 mm of Sta. 2, because comprehensive data (i.e., PLFA depth profiles) were lacking otherwise. At day 2, 60% of the label was in the algae, 12% in bacteria, <0.1% in the nematodes, and 28% in other compartments. At the end of the experiment, 45% of the ^{13}C was stored in algae, again 12% in bacteria, 0.2% in the nematodes, and 2.4% in the macrofauna. At the end of the experiments, the partitioning of ^{13}C uptake among benthic size classes (bacteria, nematodes, and macrofauna) closely follows that of carbon stocks (Fig. 8).

Discussion

Before discussing the results, it is instructive to reiterate and evaluate the experimental approach. The pulse-chase experiments have been done in situ rather than in recovered cores or in the laboratory so as to minimize disturbance. Frames had been installed to delineate the ^{13}C-enriched plots and to prevent subsurface lateral exchange. In situ, field experimentation was required to study mixing of ^{13}C-labeled material to greater depth because of physical mixing and bioturbation and to include the loss of label due to resuspension processes. Mixing and resuspension processes depend on the bottom water current velocities and wave activities, which are not easily reproduced in the laboratory.

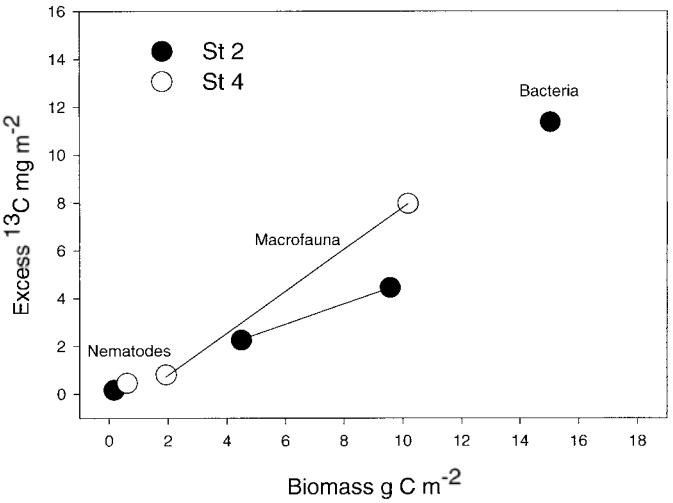

Fig. 8. Relation between biomass of heterotrophs and their ^{13}C assimilation in the upper 2 cm at Sta. 2 and Sta. 4. Macrofauna biomass and ^{13}C assimilation are presented for the upper 2 cm (lower values) and the upper 14 cm (upper values), which are connected by tie-lines.

Moreover, inclusion of macrofaunal mixing and label uptake precluded use of small diameter core incubations. In situ experimentation also limited possible changes in the behavior of organisms due to laboratory conditions deviating from field conditions.

The pulse-chase experiments provided essential, simultaneous information on label incorporation, loss, mixing, and transfer between organisms and compartments in the sediments; however, other approaches or technologies may be preferred if data on a single aspect are required. For instance, if accurate measurement of microphytobenthos production is the only objective, it would be better to use the oxygen microelectrode method (Revsbech and Jørgensen 1983), but scaling up these fine-scale measurements to areal rates of net carbon input is not straightforward. Similarly, small-core incubations with percolation of labeled bicarbonate may have been better to quantify microphytobenthos carbon fixation (Jönsson 1991) and incubations with darkened and poisoned controls to quantify meiofauna grazing (Montagna 1984, 1993). However, such treatments in small cores would not allow inclusion of macrofauna mixing and uptake, nor resuspension of sediments with associated microflora and fauna.

Label fixation and loss—Label incorporation was linear (Fig. 2), indicating that the ^{13}C:^{12}C ratio of the dissolved inorganic carbon pool was not changing significantly during incubations, which was consistent with observations during core incubations (Blanchard 1991; Jönsson 1991). ^{13}C fixation rates in the top millimeter of the sediments were identical (about 27 m^{-2} h^{-1}) but a factor of 2 to 4 lower than total carbon fixation rates in the top millimeter on the basis of ^{14}C slurry incubations. The ^{14}C-based fixation rates are potential estimates because the algae are resuspended during slurry incubations, and all nutrient gradients are destroyed (Barranguett et al. 1998). The ^{13}C fixation rates refer only to ^{13}C incorporation and could be either too low because of isotope dilution or too high because of addition of the ^{13}C spike-enhanced levels of bicarbonate, which may have induced a bias if bicarbonate availability was limiting. The net effect of these potential biases depends on the duration of incubation and actual time and depth of carbon fixation and is difficult to quantify. It is likely limited because ^{13}C fixation rates were lower than total carbon fixation rates on the basis of ^{14}C. Whatever potential bias, the partitioning and loss rates of ^{13}C are independent of actual accuracy of carbon fixation rates.

Whereas microphytobenthos production was similar, surface and integrated Chl *a* concentrations at Sta. 4 were significantly lower than those at Sta. 2 (Fig. 3C). Microscopic investigation of microphytobenthos also revealed lower biomass at Sta. 4 than at Sta. 2 (Hamels et al. 1998). The biomass to production (BP) ratio, a measure of algal turnover time, was estimated using a carbon to Chl *a* conversion factor of 40 and a primary production period of 6 h d^{-1}. BP ratios in the surface millimeter and the entire sediment are consequently lower at Sta. 4 (1.3 and 1.6 d, respectively) than at Sta. 2 (9.4 and 10.9 d, respectively). For the surface layer at Sta. 2, algal biomass and production have also been calculated from PLFA concentration and labeling patterns, and an identical BP ratio (9.5) was obtained. Turnover of algae in these tidal sediments is similar to that in other tidal flats and subtidal sediments (BP ratios of 2 to 44 d; Admiraal et al. 1982, Sundbäck et al. 1996).

Intact Chl *a* was found to 8 cm, the maximum depth sampled (Fig. 3C). This was consistent with previous studies (Steel and Baird 1968; Cadee and Hegeman 1974; Joint 1978). The gradient of Chl *a* with depth was significantly higher at Sta. 4 than at Sta. 2 (Fig. 3C). Consistently, Barranguet et al. (1997) reported steeper Chl *a* slopes with depth for sandy sites at the margin of the tidal flat than for silty sites in the central part. The Chl *a* gradient is proportional to mixing and inversely proportional to the degradation constant (Sun et al. 1991). The steeper slope at Sta. 4 relative to Sta. 2 could be due to lower mixing or higher degradation. At Sta. 4, mixing of ^{13}C-labeled algae is faster and more extensive than at Sta. 2 (Fig. 3). Degradation of Chl *a* at Sta. 4 is consequently higher than at Sta. 2; however, concentrations of pheophorbides and pheophytins (the main Chl *a* degradation products) at Sta. 4 are lower than those at Sta. 2 (Hamels et al. 1998; Lucas and Holligan 1999). High physical and biological mixing, which causes resuspension, likely prevented accumulation of these degradation products.

After the 4-h labeling period, a significant fraction of the label was found below the photic zone (Fig. 3), in particular at Sta. 4. Mixing processes can be quantified by using a simple model incorporating a pulse input of microphytobenthos material, one-dimensional diffusive transport, and first-order loss of ^{13}C:

$$C = \frac{M \exp(-kt)}{\sqrt{\pi DT}} \exp\left(-\frac{x^2}{4Dt}\right)$$

where C is the concentration of excess ^{13}C, M is the pulse input of ^{13}C (mg m^{-2}), k is the first-order loss term due to respiration and resuspension, t is time, x is depth in sedi-

ment, and D is the mixing coefficient. Fitting the day 3 data to this model yielded D values of 4 and >1000 $cm^2\ yr^{-1}$ and k values of 0.02 and 0.05 h^{-1} at Sta. 2 and Sta. 4, respectively. Although these estimates are not well constrained, it is clear that mixing and label losses are higher at Sta. 4 than at Sta. 2. Our ^{13}C-based mixing coefficient at Sta. 2 (4 $cm^2\ yr^{-1}$) is similar to that based on ^{7}Be (6.2 $cm^2\ yr^{-1}$) during June 1997 (S. Schmidt pers. comm.).

The rapid transport of label to depth may be due to active migration of benthic algae, bioturbation by deposit feeders, movement of benthic algae with draining interstitial water, or ^{13}C bicarbonate uptake by chemoautotrophs. The latter explanation would argue that deeper label penetration and more chemoautotrophy occurred at Sta. 2 relative to Sta. 4 (because of higher oxygen uptake rates at Sta. 2), whereas the reverse is observed. Moreover, recent dedicated experiments revealed nonsignificant ^{13}C bicarbonate uptake in the dark at Sta. 4. Migration of benthic algae is well known to be rapid, with an amplitude of a few millimeters in mud flats and up to 12 cm in sand flats (Kingston 1999). Deposit feeders and large meiofauna are more abundant at Sta. 4 than at Sta. 2 and may consequently more rapidly and extensively mix the sediment (Webb and Montagna 1993; Herman et al. 2000). Pore water drainage was observed at Sta. 4, but there are no indications for significant drainage at Sta. 2.

Mixing was more extensive after a few tides, and even subsurface peaks appeared (Fig. 3), perhaps due to nonlocal transport sensu Boudreau (1986). Nonlocal transport has been invoked to explain subsurface peaks in profiles of radionuclides (Smith et al. 1986; Soetaert et al. 1996), chlorophyll (Boon and Duineveld 1998), and ^{13}C-labeled algae (Blair et al. 1996). These subsurface peaks may be the result of a number of mechanisms, including subsurface defecation by surface-feeding animals and scraping of surficial material into burrows (Boudreau 1986). Mixing of labeled material can also be due to particle redistribution caused by wave and current activities (de Jonge and van Beusekom 1995) and transport of algae due to pore-water advection (Huettel et al. 1996). These physical mixing processes are more important at Sta. 4 than Sta. 2 because of higher bottom shear stresses (1.15 vs. 0.30 Pa) and lower silt contents (4 vs. 38%).

The more dynamic environment at Sta. 4 is also reflected in the higher loss of label with time (Fig. 4). The half-lives with respect to external losses were 2.4 and 5.6 d at Sta. 4 and Sta. 2, respectively. Loss of ^{13}C is mainly due to respiration and resuspension, though some material may have mixed below the maximum depth of sampling. A first-order estimate on the relative importance of respiration and resuspension losses can be obtained by constructing a carbon budget. The total amount of ^{13}C fixed must be balanced by the amount of ^{13}C recovered at the end of the experiments in the sediment and organisms; the quantity respired by macrofauna, nematodes, and other organisms; and the amount resuspended. The first part of the balance has been measured, the second part can be estimated, and resuspension can then be calculated by difference (Fig. 9). Respiration was scaled to match all losses at Sta. 2. The respiration to ^{13}C biomass ratio derived for Sta. 2 (0.42) was then imposed at Sta. 4. This tentative budget suggests that at Sta. 4, resuspension of ^{13}C (85 mg m^{-2}) removes about 34% of the label and accounts for about 64% of the total loss from the sediments (Fig. 9). These numbers represent approximate minimum estimates, because any resuspension at site two is incorporated in the respiration coefficient applied to Sta. 4. Lucas et al. (2000) have examined resuspension of microphytobenthos using annular flume experiments. At current velocities representative for the field (15 to 30 cm s^{-1}), resuspension, expressed as percentage of Chl *a* resuspended from the top 2 mm, ranged from −0.36 to 3.96% at Sta. 2 and from 11.5 to 24.6% at Sta. 4. These annular flume experimental results are consistent with our simple budget calculations on the basis of the in situ labeling experiment.

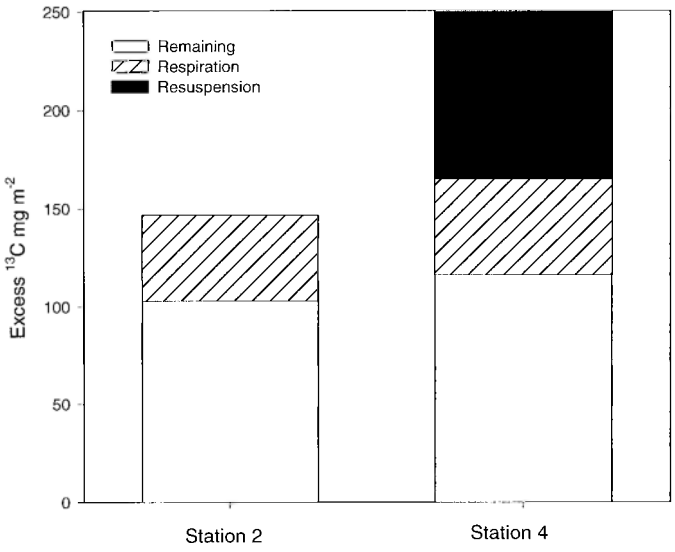

Fig. 9. Budget of excess ^{13}C for Sta. 2 (4 d) and Sta. 4 (3 d).

Data presented here indicate that similar rates of microphytobenthos production can be consistent with large differences in microphytobenthos stock and dynamics. At the sandy Sta. 4, algal biomass is low, turnover with respect to production is high (BP ratio of 1.3 to 1.6 d), and label loss with a half-life of 2.4 d is due to resuspension (60%) and respiration (40%). At the more silty Sta. 2, algal biomass is relatively high, but its renewal (BP ratio of 9.4 to 10.9 d) and removal rates (half-life of 5.6 d) are lower. Our experiments were performed in June during a period with calm weather and may not necessarily be representative for other seasons because of differences in wind speed–induced resuspension, sedimentary silt contents, and benthic community composition. However, if this uncoupling of areal productivity and biomass is a general phenomena, this will complicate the application of bio-optical models of benthic productivity.

Label transfer—The transfer from algae to bacteria and nematodes was rapid (Figs. 5, 7), because label incorporation by these heterotrophs was already detected during the period of microphytobenthos labeling. In the top 5 mm of the sediment at Sta. 2, diatoms and bacteria accounted for about 59 and 1.7%, respectively, of the total ^{13}C fixed at the end of the labeling period. The missing 39% may be a result of accumulated errors in the integration procedures, because of

high spatial variability and because total ^{13}C data are available at higher resolution than PLFA ^{13}C data. Some ^{13}C may be incorporated in microfauna and meiofauna, but this is probably a very minor fraction on the basis of their biomass (Fig. 8). The mismatch may also be due to uncertainty in the conversion factor. The PLFA concentrations were converted into diatom biomass estimates by using 0.035 g of carbon PLFA per grams of carbon biomass (Volkman et al. 1989). There are very limited data on the accuracy of this factor and how it may change with diatom growth stage. Benthic diatoms are likely to experience unbalanced growth, and a considerable part of the carbon fixed may temporarily be stored within the algae or be exudated (Smith and Underwood 1998). Recent studies indicate that extracellular organic carbon constitutes a major part of the carbon fixed by microphytobenthos (42–73%, Goto et al. 1999; 36–70%, Smith and Underwood 2000), consistent with our estimate of about 39%. These exudates may provide a direct link between algae and bacteria (Murray et al. 1986) and may explain both the rapid (within 4 h) and steady (over the first 24 h) labeling of bacteria. If the total pool of uncharacterized ^{13}C (47 mg m^{-2}) would be available to heterotrophic bacteria, they have to grow with an efficiency of about 50% to obtain the maximum ^{13}C-labeled bacterial biomass of 20 mg m^{-2}. The estimated bacterial growth efficiency is at the upper end for eutrophic waters but in the lower range for organic carbon excreted by phytoplankton (Del Giorgi and Cole 1998). Hence rapid, direct linkage between algae and bacteria may occur via exudates. Smith and Underwood (1998) have reported rapid bacterial consumption of colloidal carbohydrates and glucan (photosynthetic storage products of diatoms).

The loss of label from the top 5 mm of the sediments at Sta. 2 was somewhat higher for the diatoms ($\tau_{1/2}$ = 1.9 d) and significantly higher for bacteria ($\tau_{1/2}$ = 1.4 d) than for the total carbon pool ($\tau_{1/2}$ = 2.5 d; Fig. 7). Loss of ^{13}C from the total carbon pool is due to resuspension, respiration, and mixing to deeper layers of the sediment. Label loss from the top 5 mm ($\tau_{1/2}$ = 2.5 d) is higher than that from the upper 8 cm ($\tau_{1/2}$ = 5.6 d), because mixing to greater depth and resuspension are relatively more important for the thin surface layer. Enhanced loss of diatom and bacterial ^{13}C relative to total ^{13}C is due to grazing or higher respiration if mixing to deeper layers and resuspension are not selective. Respiration losses from the total ^{13}C pool are likely due to bacteria and algae as well because they dominate the living biomass. Consequently, grazing, lysis, and other losses than respiration contribute to enhanced loss of diatoms (0.003 ± 0.005 h^{-1}) and bacteria (0.009 ± 0.005 h^{-1}) relative to the total ^{13}C pool. These loss rates are within reported range for meiofauna grazing rates (Montagna 1984, 1995). Nematodes rapidly assimilated ^{13}C with uptake apparent after 1 h already (Fig. 5). This indicates that photosynthetically fixed ^{13}C entered the microbial food web within hours, consistent with reports by Montagna (1984). Specific uptake stabilized (Sta. 2) or decreased (Sta. 4) between the end of the labeling period and day 1. This is likely due to horizontal heterogeneity. Alternatively, the initial ^{13}C uptake may be due to grazing on labeled algae or utilization of algal exudates. The continuing assimilation of ^{13}C after 1 d could then be due to grazing on ^{13}C-labeled bacteria.

The rapid ^{13}C enrichment of nematodes was not only restricted to the upper centimeter, but was also found in the deeper layers. This rapid subsurface ^{13}C enrichment was in particular evident for *Enoploides* after 2 h. Rudnick (1989) has reported similar specific ^{14}C activities for nematodes within the upper 6 cm of the Marine Ecosystems Research Laboratories (MERL) microcosm sediments, but no information on the short-term dynamics was provided. Levin et al. (1997) observed that nematodes from 2 to 5 cm and 5 to 10 cm were enriched 1.5 d after addition of ^{13}C-labeled diatom. They attributed enrichment at depth to the presence of labeled diatoms in Maldanide tubes. In our sediments, the rapid appearance of ^{13}C-labeled nematodes occurred at depths where the bulk sediments were not yet labeled. This may indicate rapid, active vertical migration of the nematodes, in particular for the large predatory nematode *Enoploides*.

The predatory behavior of *Enoploides* has been well documented on the basis of morphology and laboratory feeding experiments (Moens et al. 1999*b*). The significant ^{13}C enrichment of *Enoploides* as early as 2 h after the start of labeling indicates that fixed ^{13}C can route within 2 h from algae over grazers to predators at the top of the microbial benthic food web. Alternatively, *Enoploides* is not an obligatory predator (as observed in laboratory feeding experiments) and may directly graze on the microalgae or consume their photosynthetic products, as has been reported for harpacticoid copepods (Decho and Moriarty 1990).

Specific labeling patterns ($\Delta\delta^{13}C$) at the end of the chase experiments were rather similar for macrofauna, nematodes (Fig. 5), and bacterial biomarkers (Fig. 6). Partitioning among these benthic size classes was consequently primarily related to their relative biomasses (Fig. 8), consistent with observations for meio- and macrofauna ^{14}C incorporation of phytoplankton (Widbom and Frithsen 1995). The biomass spectrum in our intertidal sediments (bacteria > macrofauna > meiofauna) is similar to that in other coastal sediments (Heip et al. 1995; Herman et al. 1999). It appears that each benthic size group profits proportionally from the carbon fixed by microphytobenthos, indicating comparable relative growth rate for each size class over the 3- to 4-d period. This is a surprising result given that production to biomass ratios for these heterotrophs vary from 1 to 2 yr^{-1} for macrofauna and 3 to 24 yr^{-1} for meiofauna, and they are higher than 100 yr^{-1} for bacteria (Heip et al. 1995). This apparent inconsistency between our observations for benthic size groups and literature production to biomass ratios for individual organisms (macrofauna and meiofauna) and bacterial communities is likely the result of the experimental time window and the variable share of microphytobenthos-depending heterotrophs to total biomass. The experimental time window (3 to 4 d) favored labeling of meiofauna (Fig. 5D), whereas macrofauna labeling is expected to be incomplete given typical tissue turnover of macrofauna (Heip et al. 1995). Similarly, bacterial labeling was maximal after 1 to 2 d (Figs. 6, 7) and decreased thereafter. The fraction of each benthic size class that directly depends on microphytobenthos is likely variable among size classes and between

sites. For instance, Herman et al. (2000) have shown that the relative importance of microphytobenthos for benthic macrofauna depends on the species involved. Specific labeling patterns of bacterial PLFA relative to algal PLFA (Fig. 6) indicate that only a fraction of the bacterial population has assimilated microphytobenthos-derived carbon. The in situ labeling approach has the potential to trace and quantify direct linkages between base and higher trophic levels (microphytobenthos, this study; phytoplankton, Blair et al. 1996, Levin et al. 1997; bacteria, Hall and Meyer 1998), but the transfer pathways (exudates vs. grazing) and organisms involved will differ.

References

Admiraal, W., H. Peletier, and H. Zomer. 1982. Observations and experiments on the population dynamics of epipelic diatoms from an estuarine mudflat. Estuar. Coast. Shelf Sci. **14:** 471–487.

Barranguet, C., P. M. J. Herman, and J. J. Sinke. 1997. Microphytobenthos biomass and community composition studied by pigment biomarkers: Importance and fate in the carbon cycle of a tidal flat. J. Sea Res. **38:** 59–70.

———, J. Kromkamp, and J. Peene. 1998. Factors controlling primary production and photosynthetic characteristics of intertidal microphytobenthos. Mar. Ecol. Prog. Ser. **173:** 117–126.

Blair, N. E., L. A. Levin, D. J. DeMaster, and G. Plaia. 1996. The short-term fate of fresh algal carbon in continental slope sediments. Limnol. Oceanogr. **41:** 1208–1219.

Blanchard, G. F. 1991. Measurement of meiofauna grazing rates on microphytobenthos: Is primary production a limiting factor? J. Exp. Mar. Biol. Ecol. **147:** 37–46.

Boon, A. R., and G. C. A. Duineveld. 1998. Chlorophyll *a* as a marker for bioturbation and carbon flux in southern and central North Sea sediments. Mar. Ecol. Prog. Ser. **162:** 33–43.

Boschker, H. T. S., J. F. C. de Brouwer, and T. E. Cappenberg. 1999. The contribution of macrophyte derived organic matter in microbial biomass in salt marsh sediments: Stable carbon-isotope analysis of microbial biomarkers. Limnol. Oceanogr. **44:** 309–319.

———, S. C. Nold, P. Wellsbury, D. Bos, W. de Graaf, R. Pel, R. J. Parkes, and T. E. Cappenberg. 1998. Direct linking of microbial populations to specific biogeochemical processes by ^{13}C-labelling of biomarkers. Nature **392:** 801–805.

Boudreau, B. P. 1986. Mathematics of tracer mixing in sediments. II Nonlocal mixing and biological conveyor-belt phenomena. Am. J. Sci. **286:** 199–238.

Brinch-Iversen, J., and G. M. King. 1990. Effects of substrate concentration, growth state, and oxygen availability on relationships among bacterial carbon, nitrogen and phospholipid phosphorus content. FEMS Microbiol. Ecol. **74:** 345–356.

Cadee, G. C., and J. Hegeman. 1974. Primary production of the benthic microflora living on tidal flats in the Dutch Wadden Sea. Neth. J. Sea Res. **8:** 260–291.

Decho, A. W., and D. J. Moriarty. 1990. Bacterial exopolymer utilization by a harpacticoid copepod: A methodology and results. Limnol. Oceanogr. **35:** 1039–1049.

De Jonge, V. N., and J. E. E. van Beusekom. 1995. Wind- and tide-induced resuspension of sediment and microphytobenthos from tidal flats in the Ems estuary. Limnol. Oceanogr. **40:** 766–778.

Del Giorgio, P. A., and J. J. Cole. 1998. Bacterial growth efficiency in natural aquatic systems. Annu. Rev. Ecol. Syst. **29:** 503–541.

Dobbs, F. C., J. B. Guckert, and K. R. Carman. 1989. Comparison of three techniques for administering radiolabeled substrates to sediments for trophic studies: Incorporation by microbes. Microbiol. Ecol. **17:** 237–250.

Goto, N., T. Kawamura, O. Mitamura, and H. Terai. 1999. Importance of extracellular organic carbon production in the total primary production by tidal-flat diatoms in comparison to phytoplankton. Mar. Ecol. Prog. Ser. **190:** 289–295.

Guckert, J. B., C. P. Antworth, P. D. Nichols, and D. C. White. 1985. Phospholipid ester-linked fatty acid profiles as reproducible assays for changes in prokaryotic community structure of estuarine sediments. FEMS Microbiol. Ecol. **31:** 147–158.

Guezennec, J., and A. Fialamedioni. 1996. Bacterial abundance and diversity in the Barbados trench determined by phospholipid analysis. FEMS Microbiol. Ecol. **19:** 83–93.

Hall, R. O., and J. L. Meyer. 1998. The trophic significance of bacteria in a detritus-based stream food web. Ecology **79:** 1995–2012.

Hamels, I., K. Sabbe, K. Muylaert, C. Barranguet, C. Lucas, P. M. J. Herman, and W. Vyverman. 1998. Organisation of microbenthic communities in intertidal estuarine flats, a case study from the Molenplaat Westerschelde Estuary, The Netherlands. Eur. J. Protistol. **34:** 308–320.

Heip, C. H. R., N. K. Goosen, P. M. J. Herman, J. Kromkamp, J. J. Middelburg, and K. Soetaert. 1995. Production and consumption of biological particles in temperate tidal estuaries. Oceanogr. Mar. Biol. Annu. Rev. **33:** 1–150.

Herman, P. M. J., J. J. Middelburg, J. van de Koppel, and C. H. R. Heip. 1999. The ecology of estuarine macrobenthos. Adv. Ecol. Res. **29:** 195–240.

———, J. J. Middelburg, J. Widdows, C. H. Lucas, and C. H. R. Heip. 2000. Stable isotopes as trophic tracers: Combining field sampling and manipulative labelling of food resources for macrobenthos. Mar. Ecol. Prog. Ser. In press.

Holland, A. F., R. G. Zingmark, and J. M. Dean. 1974. Quantitative evidence concerning the stabilization of sediments by marine benthic diatoms. Mar. Biol. **27:** 191–196.

Huettel, M., W. Ziebis, and S. Forster. 1996. Flow-induced uptake of particulate matter in permeable sediments. Limnol. Oceanogr. **41:** 309–322.

Joint, I. R. 1978. Microbial production of an estuarine mudflat. Estuar. Coast. Mar. Sci. **7:** 185–195.

Jönsson, B. 1991. A ^{14}C incubation technique for measuring microphytobenthic primary productivity in intact sediment cores. Limnol. Oceanogr. **36:** 1485–1492.

Kingston, M. B. 1999. Wave effects on the vertical migration of two benthic microalgae: *Hantzschia virgata* var. *intermedia* and *Euglena proxima.* Estuaries **22:** 81–91.

Kromkamp, J., C. Barranguet, and J. Peene. 1998. Determination of microphytobenthos PSII quantum efficiency and photosynthetic activity by means of variable chlorophyll fluorescence. Mar. Ecol. Prog. Ser. **162:** 45–55.

Levin, L., N. Blair, D. DeMaster, G. Plaia, W. Fornes, and C. Martin. 1997. Rapid subduction of organic matter by maldanid polychaetes on the North Carolina slope: A keystone phenomenon? J. Mar. Res. **55:** 595–611.

Lucas, C. H., and P. M. Holligan. 1999. Nature and ecological implications of algal pigment diversity on the Molenplaat tidal flat Westerschelde estuary. Mar. Ecol. Prog. Ser. **180:** 51–64.

———, J. Widdows, M. D. Brinsley, P. N. Salkeld, and P. M. J. Herman. 2000. Benthic-pelagic exchange of microalgae at a tidal flat. 1. Pigment analysis. Mar. Ecol. Prog. Ser. **196:** 59–73.

MacIntyre, H. L., and J. J. Cullen. 1995. Fine-scale vertical resolution of chlorophyll and photosynthetic parameters in shallow-water benthos. Mar. Ecol. Prog. Ser. **122:** 227–237.

———, R. J. GEIDER, AND D. C. MILLER. 1996. Microphytobenthos: The ecological role of the "secret garden" of unvegetated, shallow-water marine habitats: I. Distribution, abundance and primary production. Estuaries **19:** 186–201.

MILLER, D. C., R. J. GEIDER, AND H. L. MACINTYRE. 1996. Microphytobenthos: The ecological role of the "secret garden" of unvegetated, shallow-water marine habitats: II. Role in sediment stability and shallow-water food webs. Estuaries **19:** 202–212.

MOENS, T., D. VAN GANSBEKE, AND M. VINCX. 1999*a*. Linking estuarine intertidal nematodes to their suspected food: A case study from the Westerschelde estuary (S.W. Netherlands). J. Mar. Biol. Ass. U.K. **79:** 1017–1027.

———, L. VERBEECK, AND M. VINCX. 1999*b*. Feeding biology of a predatory and a facultatively predatory marine nematode *Enoploides longispiculosus* and *Adoncholaimus fuscus*). Mar. Biol. **134:** 585–593.

———, L. VERBEECK, AND M. VINCX. 1999*c*. Preservation- and incubation time–induced bias in tracer-aided grazing studies on meiofauna. Mar. Biol. **133:** 69–77.

MONTAGNA, P. A. 1984. In situ measurement of meiobenthic grazing rates on sediment bacteria and edaphic diatoms. Mar. Ecol. Prog. Ser. **18:** 119–130.

———. 1993. Radioisotope technique to quantify in situ microbivory by meiofauna in sediments, p. 745–753. *In* P. F. Kemp, B. F. Sherr, E. B. Sherr, and J. J. Cole [eds.], Handbook of methods in aquatic microbial ecology. Lewis.

———. 1995. Rates of metazoan meiofaunal microbivory: A review. Vie Milieu **45:** 1–9.

MURRAY, R. E., K. E. COOKSEY, AND J. C. PRISCU. 1986. Stimulation of bacterial DNA synthesis by algal exudates in attached algal-bacterial consortia. Appl. Environ. Microbiol. **52:** 1177–1182.

PATERSON, D. M., AND K. S. BLACK. 1999. Water flow, sediment dynamics and benthic biology. Adv. Ecol. Res. **29:** 155–193.

RAJENDRAN, N., O. MATSUDA, Y. URUSHIGAWA, AND U. SIMIDU. 1994. Characterization of microbial community structure in the surface sediment of Osaka Bay, Japan, by phospholipid fatty acid analysis. Appl. Environ. Microbiol. **60:** 248–257.

———, Y. SUWA, AND Y. URUSHIGAWA. 1993. Distribution of phospholipid ester-linked fatty acid biomarkers for bacteria in the sediment of Ise Bay, Japan. Mar. Chem. **42:** 39–56.

REVSBECH, N. P., AND B. B. JØRGENSEN. 1983. Photosynthesis of benthic microflora measured with high spatial resolution by the oxygen microprofile method: Capabilities and limitations of the method. Limnol. Oceanogr. **28:** 749–756.

RISGAARD-PETERSEN, N., S. RYSGAARD, L. P. NIELSEN, AND N. P. REVSBECH. 1994. Diurnal variation of denitrification and nitrification in sediments colonized by benthic microphytes. Limnol. Oceanogr. **39:** 573–579.

RUDNICK, D. T. 1989. Time lags between the deposition and meiobenthic assimilation of phytodetritus. Mar. Ecol. Prog. Ser. **50:** 231–240.

SMITH, D. J., AND G. J. C. UNDERWOOD. 1998. Exopolymer production by intertidal epipelic diatoms. Limnol. Oceanogr. **43:** 1578–1591.

———, AND G. J. C. UNDERWOOD. 2000. The production of extracellular carbohydrates by estuarine benthic diatoms: The effects of growth phase and light and dark treatment. J. Phycol. In press.

SMITH, J. N., C. T. SCHAFFER, B. P. BOUDREAU, AND V. NOSHKIN. 1986. Plutonium and ^{210}Pb distributions in northeast Atlantic sediments: Subsurface anomalies caused by non-local mixing. Earth Planet. Sci. Lett. **81:** 15–28.

SOETAERT, K., AND OTHERS. 1996. Modelling ^{210}Pb-derived mixing activity in ocean margin sediments: Diffusive versus non-local mixing. J. Mar. Res. **54:** 1207–1227.

STEELE, J. H., AND I. E. BAIRD. 1968. Production ecology of a sandy beach. Limnol. Oceanogr. **13:** 14–25.

STEWARD, C. C., S. C. NOLD, D. B. RINGELBERG, D. C. WHITE, AND C. R. LOVELL. 1996. Microbial biomass and community structures in the burrows of bromophenol producing and nonproducing marine worms and surrounding sediments. Mar. Ecol. Prog. Ser. **133:** 149–165.

SUN, M., R. C. ALLER, AND C. LEE. 1991. Early diagenesis of chlorophyll-*a* in Long Island Sound sediments: A measure of carbon flux and particle reworking. J. Mar. Res. **49:** 379–401.

SUNDBÄCK, K., P. NILSSON, C. NILSSON, AND B. JÖNSSON. 1996. Balance between autotrophic and heterotrophic components and processes in microbenthic communities of sandy sediments: A field study. Estuar. Coast Shelf Sci. **43:** 689–706.

UNDERWOOD, G. J. C., AND J. KROMKAMP. 1999. Primary production by phytoplankton and microphytobenthos in estuaries. Adv. Ecol. Res. **29:** 93–153.

VOLKMAN, J. K., S. W. JEFFREY, P. D. NICHOLS, G. I. ROGERS, AND C. D. GARLAND. 1989. Fatty acid and lipid composition of 10 species of microalgae used in mariculture. J. Exp. Mar. Biol. Ecol. **128:** 219–240.

WEBB, D. B., AND P. A. MONTAGNA. 1993. Initial burial and subsequent degradation of sedimented phytoplankton: Relative impact of macro- and meiobenthos. J. Exp. Mar. Biol. Ecol. **166:** 151–163.

WIDBOM, B., AND J. B. FRITHSEN. 1995. Structuring factors in a marine soft bottom community during eutrophication—an experiment with radiolabelled phytodetritus. Oecologia **101:** 156–168.

Received: 12 October 1999
Accepted: 1 May 2000
Amended: 15 May 2000